

ab initio frame transformation calculations of direct and indirect dissociative recombination rates of $\text{HeH}^+ + e^-$

Daniel J. Haxton^{1,*} and Chris H. Greene^{1,†}

¹*Department of Physics and JILA, University of Colorado, Boulder Colorado 80309*

The HeH^+ cation undergoes dissociative recombination with a free electron to produce neutral He and H fragments. We present calculations using *ab initio* quantum defects and Fano's rovibrational frame transformation technique, along with the methodology of Ref. [1], to obtain the recombination rate both in the low-energy (1-300 meV) and high-energy (ca. 0.6 hartree) regions. We obtain very good agreement with experimental results, demonstrating that this relatively simple method is able to reproduce observed rates for both indirect dissociative recombination, driven by rovibrationally autoionizing states in the low-energy region, and direct dissociative recombination, driven by electronically autoionizing Rydberg states attached to higher-energy excited cation channels.

PACS numbers: 03.65.Nk, 34.80.-i, 34.80.Lx, 33.20.Wr

I. INTRODUCTION

The dissociative recombination (DR)[2, 3, 4] reaction $\text{HeH}^+ + e^- \rightarrow \text{He} + \text{H}$ has received considerable theoretical and experimental interest. HeH^+ ion chemistry is important to the understanding of the composition of interstellar space. Observations [5] have failed to show much HeH^+ present in the interstellar medium, and were in contradiction to the early prediction [6] that this species would be abundant. These observations indicated that the low-energy DR cross section of $\text{HeH}^+ + e^-$ is indeed significant, though there is no valence electronic state of the neutral that provides a mechanism for the high rate at low collision energy.

Thus, much theoretical and experimental interest has been focused on this process in the intervening years. Experiments [7, 8, 9, 10, 11, 12, 13, 14] show peaks in the DR cross section in both the low-energy region (ca. 1-300 meV) and the high-energy region around 20 eV. It is the low-energy peak that is responsible for the destruction of HeH^+ in interstellar space.

The low and high energy peaks are caused by two different mechanisms, the indirect and direct, respectively. The indirect mechanism has proved more difficult to treat theoretically, and the initial underestimate [6] of the low-energy DR rate was based upon a consideration of the direct mechanism only.

The presence of the two mechanisms, and the importance of this process to the understanding of interstellar chemistry, makes the DR of HeH^+ a prime target for theory. Several treatments [2, 14, 15, 16, 17, 18, 19] have been presented, and these have had varying success at reproducing experimental DR rates. The study of Orel *et al.* [15] reproduced the magnitude and size of the high-energy peak, but did not accurately reproduce the shoulder on the high-energy side. Takagi [18, 19] has

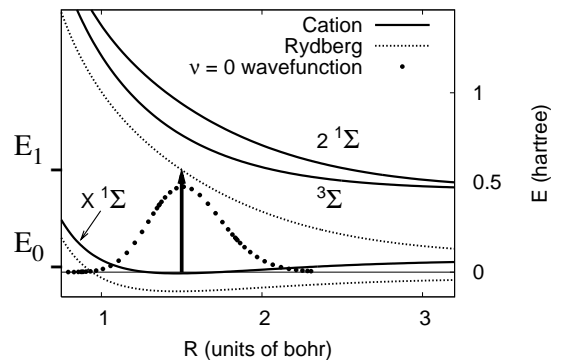


FIG. 1: Schematic of HeH^+ DR. The ground rovibrational state of the cation is plotted as dots; the cation curves, as solid lines; and Rydberg curves supported by the lowest and highest cation curves, as dotted lines. Typical incident electron energies for the low-energy and high-energy DR are labeled E_0 and E_1 , respectively.

obtained good agreement for the low-energy peak, but did not reproduce all the peaks and dips in the cross section perfectly.

As schematic of the process is shown in Fig. 1. Indirect DR[2] in the low-energy region is driven by transitions to rovibrationally autoionizing Rydberg states supported by the lowest cation curve. Such states are described as a Rydberg electron attached to a rotationally or vibrationally excited, but electronically ground-state, HeH^+ cation core. The DR process is driven by nonadiabatic coupling to and among these Rydberg states. The DR cross section exhibits peaks corresponding to the locations of the autoionizing resonances, which serve as doorways.

The direct DR process[20, 21] is driven by a transfer of energy among the electronic degrees of freedom only: an incident electron with sufficient energy may excite the ground-state ($1\ \Sigma$) HeH^+ cation core, such that the incident electron becomes trapped in a Rydberg state supported by a dissociative σ cation core. This is a vertical

*Electronic address: dhaxton@jila.colorado.edu

†Electronic address: chris.greene@colorado.edu

transition, labeled by an arrow in Fig. 1, and nonadiabatic coupling is unimportant to the total DR rate. Once the electronic transition to the metastable Rydberg state has occurred, the molecule follows the dissociative Rydberg potential energy surface toward breakup. Our studies indicate that most of the high-energy DR to HeH^+ is accounted for by the Rydberg series converging to the upper singlet curve.

II. THEORY

Several theoretical methodologies have found reasonable success in treating the dissociative recombination of HeH^+ , but there is still room for improvement. Treatments[15, 16, 17] using the formalism of O'Malley[21], in which the DR rate is obtained by calculating potential energy curves of the autoionizing Rydberg states of HeH , may be contrasted with treatments[14, 18, 19] using multichannel quantum defect theory (MQDT)[22, 23, 24, 25, 26] in which the only potential energy curves explicitly included are those of the cation, or those in which both cation and neutral curves are used [2, 27]. Scattering calculations using vibrational close coupling were used in Ref. [28].

The O'Malley treatment was used by Orel *et al.*[15] to calculate the high energy peak; those authors reproduced the magnitude and basic shape of the high-energy peak obtained from the 1993 experiment of Sundstrom *et al.*[9] by including a total of eight doubly excited Rydberg states (six Σ and two Π). To calculate the low-energy peak under the O'Malley framework, Larson *et al.*[16] required nonadiabatic coupling matrix elements between the ground and Σ -core Rydberg states of HeH^+ ; their study underestimated the magnitude of the experimental result by a factor of ten to 100.

Treatments using multichannel quantum defect theory can be considerably simpler than those using the O'Malley treatment because they do not necessarily require the enumeration of the Rydberg states contributing to the process. Such treatments include ours and those of Takagi [18, 19] and Guberman [2]. The main difference between our method and those of Takagi and Guberman is that ours includes the DR process in the closed channel space of the MQDT calculation, whereas the others include DR channels in the open channel space.

Guberman's pioneering 1994 paper [2] employed the hybrid technique [27] incorporating both dissociative neutral and cation curves. In this method one typically has dissociative valence states and MQDT S-matrices corresponding to the Rydberg series, and one proceeds by coupling these in the first Born approximation. The coupling can be purely electronic or can arise from nonadiabatic coupling.

Nonadiabatic coupling was employed in Guberman's treatment. He defined MQDT S-matrices using the curve of the D state of neutral HeH . He treated the C state, which lies below the D state, as an open dissociative chan-

nel. The C and D states avoid and the nonadiabatic coupling between them is included as the discrete-continuum coupling as in Ref. [27].

Guberman's technique has several advantages, notably that it incorporates the correct asymptotic form of the wavefunction. However, it requires the identification of the dominant final electronic state channel of the DR process before doing the calculation, and thus may be difficult to apply to a general problem.

Our method of calculating DR rates using MQDT is similar to Takagi's method[18, 19] in that it incorporates a vibrational frame transformation[23, 24] including both bound and continuum vibrational wavefunctions of the HeH^+ cation. Our methods differ in the choice and treatment of the continuum vibrational states. Takagi employs standing-wave boundary conditions (box states), and chooses a subset of these states to represent the DR channels, interspersed among others that are chosen to be closed. We employ outgoing-wave boundary conditions[1], and consider such continuum channels open or closed according to the real part of their complex-valued energies. Thus, in our method, the DR channels are not explicitly included in the calculated s-matrix, whereas in Takagi and Guberman's treatments, they are.

Whereas Guberman's calculation incorporates the correct asymptotic form of the wavefunction, but is difficult to implement for a general system, our method and that of Takagi incorporate unphysical boundary conditions and are more easy to implement. In Takagi's treatment, some box continuum states are chosen to be open and some closed, and these are interspersed among each other. Therefore, in some box states the bound-state boundary condition is imposed for the electron, and for others, they are not. The calculation has Rydberg states attached to closed box states and this situation is clearly unphysical. In our calculation, we have wavefunctions with complex energy, asymptotically increasing at large bond length, which is also clearly unphysical. However, in the limit that the discretized continuum states have a negligibly small imaginary component to their energy, our wavefunction corresponds to the correct physical scattering wavefunction having outgoing wave boundary conditions in the diatomic coordinate.

At present, our method has not been applied to the problem of the final-state distribution of the electronic states of the fragment atoms. Applying the methods of Guberman or Takagi to this problem is more straightforward than it is for our method.

A. Outgoing wave basis functions

The original outline of our method[1] as well as subsequent calculations of DR rates for physical systems[29, 30, 31] used the technique of Siegert pseudostates[32] to define the outgoing-wave cation vibrational basis. However, there are a few difficulties with the formal theory

presented in these papers that we would like to address. The Siegert-state basis is orthonormal with respect to integration plus a surface term,

$$\int dR \chi_\alpha(R)\chi_\beta(R) + i\frac{\chi_\alpha(R_0)\chi_\beta(R_0)}{k_\alpha + k_\beta} = \delta_{\alpha\beta}, \quad (1)$$

where k_α is the Siegert pseudostate wavenumber eigenvalue for state number α . By analogy, the frame-transformed S-matrix has been written (see, for example, Eq.(6) in Ref. [1])

$$S_{\alpha\beta} = \int dR \chi_\alpha(R)s(R)\chi_\beta(R) + i\frac{\chi_\alpha(R_0)s(R_0)\chi_\beta(R_0)}{k_\alpha + k_\beta}. \quad (2)$$

However, questions may be raised as to whether this *ad hoc* expression represents the proper transformation of the S-matrix from the R basis to the χ basis. For instance, this equation does not preserve the eigenphases of the MQDT s-matrix, and is not invertible.

The orthonormality properties of the Siegert pseudostates are well known[32], and it is not hard to derive a more appropriate expression for the transformed S-matrix using Siegert pseudostates. However, in the present paper we choose to use a different method to enforce outgoing-wave boundary conditions in the vibrational basis.

Complex absorbing potentials (CAP) [33, 34, 35] or exterior complex scaling (ECS)[36, 37, 38, 39, 40, 41, 42] are alternative methods of defining outgoing-wave states. The set of eigenvectors obtained from these methods obey a simpler orthonormality relationship than do the Siegert pseudostates: they may be chosen orthonormal with respect to the inner product in which neither the bra nor ket is complex-conjugated, called the C-norm,

$$\int dR \chi_\alpha(R)\chi_\beta(R) = \delta_{\alpha\beta}. \quad (3)$$

Unlike the orthonormality relationship of the Siegert states, the C-norm is an inner product and defines the ECS or CAP states as basis vectors of a vector space. The frame transformation of the fixed-nuclei S-matrix to the ECS or CAP basis uses this inner product and is straightforward:

$$S_{\alpha\beta} = \int dR \chi_\alpha(R)s(R)\chi_\beta(R). \quad (4)$$

This transformation preserves the eigenphases exactly in the complete-basis limit. We then apply the rotational frame transformation of Ref.[24].

Previous applications of the method outlined in Ref. [1] have been on indirect DR in which electron-impact dissociation is not energetically open. Thus, the outgoing-wave vibrational states have corresponded to closed channels in these studies. In contrast, for the present analysis of the high-energy peak in HeH^+ DR, electron-impact

dissociation to $\text{H}^+ + \text{He}$ is energetically open (that to $\text{H} + \text{He}^+$ may be) and we have outgoing-wave vibrational functions as open channels.

It is worth mentioning that in either case, the asymptotic form of the wavefunction is unphysical, because of the presence of outgoing wave basis functions with complex energy that are exponentially increasing in magnitude. For the frame-transformed S-matrix in the c-normed vibrational basis, each column of which corresponds to an outgoing-wave scattering state $\Psi^{+(i)}$,

$$\Psi_\alpha^+ = \chi_\alpha(R)h_{l_\alpha}^-(k_\alpha r) + \sum_\beta S_{\alpha\beta}\chi_\beta(R)h_{l_\beta}^+(k_\beta r), \quad (5)$$

the proper statement of unitarity easily is found not to be

$$\forall_\alpha \sum_\beta |S_{\alpha\beta}|^2 = 1 \quad (6)$$

but

$$\forall_\alpha \sum_{\beta\gamma} S_{\alpha\beta}U_{\beta\gamma}S_{\alpha\gamma}^* = 1 \quad (7)$$

where

$$U_{\beta\gamma} = \int dR \chi_\beta(R)\chi_\gamma(R)^*. \quad (8)$$

While it is easy to prove that the frame-transformed and channel-closed S-matrix with bound states is unitary in the complete basis limit, we have no proof that our constructed S-matrix is guaranteed to be subunitary, though we have found this to be the case in the applications of this theory to date.

Thus, the outline of the calculation is as follows. We calculate fixed-nuclei S-matrices $s_{lm,l'm'}(R)$ and transform them to the ECS basis via Eq.(4). We then apply the rotational frame transformation of Chang and Fano [24]. We finally apply the channel-closing formula,

$$\mathcal{S}(E) = S_{oo} - S_{oc} \left(S_{cc} - e^{-2i\beta(E)} \right)^{-1} S_{co} \quad (9)$$

$$\beta(E) = \frac{\pi\delta_{\alpha\beta}}{\sqrt{2(E_\alpha - E)}},$$

where the subscript c and o denote the closed and open channel subblocks of the MQDT S-matrix S , α is now a collective index including angular momentum quantum numbers, and we introduce the notation \mathcal{S} for the physical S-matrix. The DR cross section is then obtained from the unitary defect of the frame-transformed S-matrix,

$$\sigma_\alpha(E) = \frac{\pi}{2E} \left(1 - \sum_{\beta\gamma} \mathcal{S}_{\alpha\beta}U_{\beta\gamma}\mathcal{S}_{\alpha\gamma}^* \right). \quad (10)$$

We Boltzmann average and convolute with respect to the parallel and transverse spreads in the incident electron energy in the experiment, as described in Ref. [31].

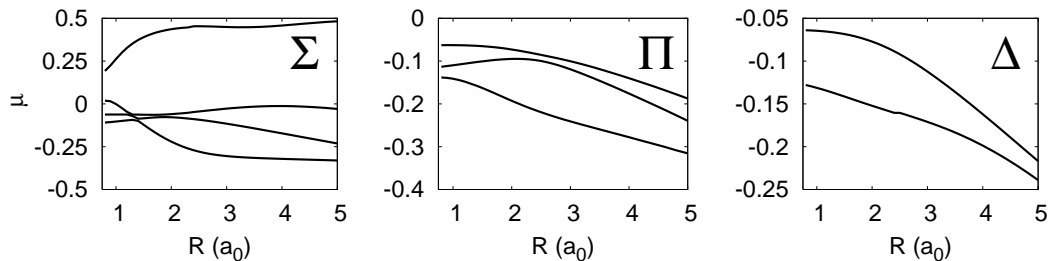


FIG. 2: Quantum eigendefects calculated at zero incident energy in the ground state cation channel.

III. CALCULATION OF *AB INITIO* QUANTUM DEFECTS AND CATION ROVIBRATIONAL STATES

We calculate quantum defects using the polyatomic UK R-matrix program[43], which is based on the Swedish-Molecule and Alchemy suites of quantum chemistry codes[44]. We include s , p , d , and f -wave basis functions (only s , p , and d for the high-energy peak) for the scattered electron in an R-matrix box of radius 14 bohr, calculated with the program GTOBAS[45]. We use the cc-pvtz basis set. For calculations on the low-energy region, we include the lone 1σ SCF orbital of HeH^+ and an additional six σ and two pairs of π virtual orbitals for the target space. The three lowest cation target states, 1 and 2 $^1\Sigma$ and $^3\Sigma$, are included in the scattering calculation and defined by full CI in the target space. Penetration terms defined by full CI of three electrons in the target space are included in the scattering wavefunction.

For the high-energy DR calculations, the HeH^+ target states are represented by full CI in the orbital space of a CASSCF calculation on the ground state, performed with the molpro quantum chemistry package[46]. Following Orel *et al.*[15], we use a total of four σ orbitals and one π orbital. We include the first three cation states and use an R-matrix radius of eight bohr. Penetration terms with full CI of three electrons are again included in the scattering wavefunction.

Quantum defects at zero incident energy in the ground-state cation channel are plotted in Fig. 2.

To perform the frame-transformation calculation to obtain the low-energy DR rate, we interpolate the calculated fixed-nuclei s-matrices over a range of $R=0.75$ to 4.5 bohr, and calculate outgoing-wave ECS vibrational states using the finite-element Gauss-Lobatto discrete variable representation [47]. We used 16-point quadrature and seven elements, scaling the R coordinate at an angle of $\frac{1}{8}\pi$ on the sixth element (the calculation is almost fully converged at 10th order quadrature). We included 42 vibrational wavefunctions; the calculations of Ref. [48] found 12 bound states, and our vibrational states include seven with real energies and ten with imaginary energy component less than 0.0001 hartree in magnitude. We use the ground-state cation potential energy surface of Coxon and Hajigeorgiou[49] and use modified atomic

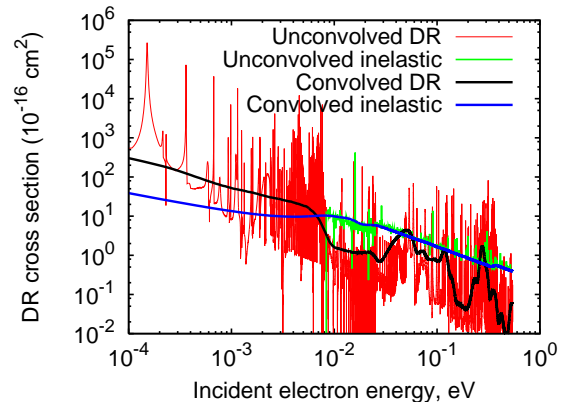


FIG. 3: (Color online) Unconvolved cross section calculated for the low-energy DR of the ground rovibrational state of ^4HeH .

weights with reduced mass

$$\mu_{eff} = \frac{m_{H\frac{1}{2}^+} m_{He\frac{1}{2}^+}}{m_{H\frac{1}{2}^+} + m_{He\frac{1}{2}^+}}, \quad (11)$$

where $m_{He\frac{1}{2}^+}$ is the mass of a helium nucleus plus one and a half electrons and $m_{H\frac{1}{2}^+}$ is the mass of a proton plus a half electron. The results are slightly sensitive to such fine-tuning (which approximately accounts for non-adiabatic coupling) and we find this choice to produce the best agreement with prior calculations of HeH^+ rovibrational spectra. For transitions up to $\nu = 3$ or $j = 3$ we find good agreement with the results of Bishop and Cheung[50], with errors less than 21 cm^{-1} .

IV. RESULTS

Results for the low-energy calculation on HeH^+ are plotted in Figs. 3, 4, and 5. Figure 3 shows the unconvolved cross section for DR of the ground rovibrational state of ^4HeH . To compare with experiment, we also convolve our results using a transverse spread of 10meV and a parallel spread of 0.1meV in the incident electron energy, to account for the experimental parameters of Ref. [14].

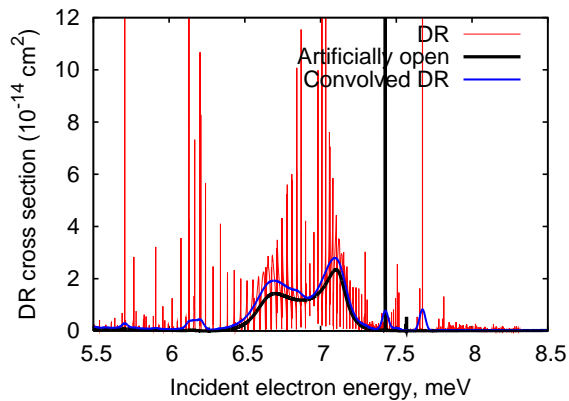


FIG. 4: (Color online) Cross section calculated in the vicinity of the $j = 1$ threshold at 8.3meV. Unconvolved physical DR cross section, red line; physical DR cross section convolved with a gaussian, purple line; unphysical cross section calculated by artificially opening the $j = 1$ channel, black line.

Inelastic scattering leads to rotational or vibrational excitation of the cation and is allowed starting at an energy of 8.3meV, where the first rotational threshold ($j = 1$) lies. As shown in Fig. 3, at that threshold there is a clear step down in the DR cross section, and the inelastic cross section assumes a value near the averaged DR rate below threshold. This finding confirms the basic picture of the indirect mechanism, and parallels our findings on the DR of LiH^+ [30, 31]. Below the $j = 1$ threshold, the only inelastic process open is dissociative recombination; above it, rotational excitation of the cation is allowed, and this process competes with DR and in fact dominates it, decreasing the DR cross section.

Thus, for energies below the $j = 1$ threshold of 8.3meV, the DR is seen to be driven by capture into Rydberg states supported by the $j = 1$ rotational state of the cation. These resonances are visible in Fig. 3 and have a sharp cut-off at the 8.3meV threshold. Another forest of Rydberg states terminates at the second excited rotational threshold, $j = 2$, at 24.9meV; at this energy, there is a dip visible in the convolved DR cross section, but a series of broad resonances then appears and increases the cross section. The inelastic cross section has only a barely visible step up at the second excited rotational threshold, showing that rotational excitation to $j = 1$ is much stronger than that to $j = 2$.

A close-up view of the calculated cross section for DR of the ground rovibrational state of ^4HeH is shown in Fig. 4. In this figure we also plot the result of calculations in which the first excited rotational channel ($j = 1$) is left open even below its threshold. Such a calculation eliminates the Rydberg series converging to the $j = 1$ threshold and reveals the presence of resonances attached to higher channel thresholds. In this figure we plot the unconvolved physical DR cross section; the physical DR cross section convolved with a gaussian to show its average value; and the unphysical, artificially-opened $j = 1$

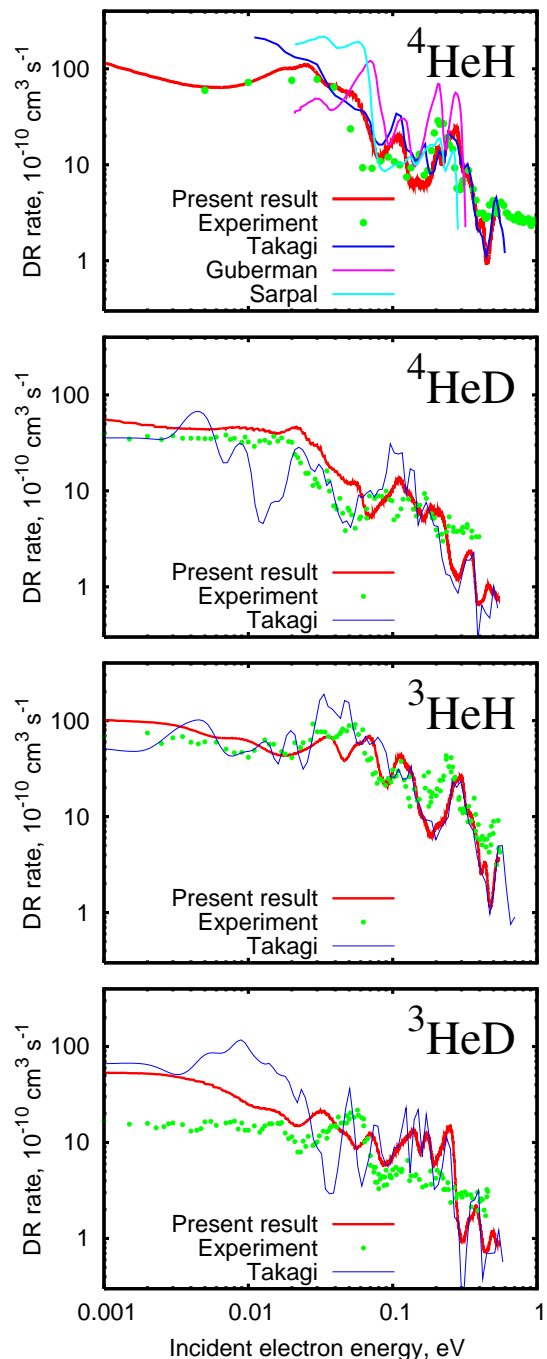


FIG. 5: (Color online) Low-energy DR rate coefficient compared with the experiment of Tanabe *et al.*[14] and the theoretical results of Takagi[14], Guberman[2], and Sarpal *et al.*[28].

channel result. Note that, as in Refs.[30, 31], there is an enhancement of the DR rate at a complex resonance, i.e., a resonance involving a lower principal quantum number state embedded in the very high Rydberg series converging to an excited cation state threshold. In contrast to Refs.[30, 31], however, the complex resonance mech-

anism is here seen to be supported by rotationally autoionizing resonances, rather than vibrationally autoionizing ones. This suggests that some of the ideas shown in Refs.[30, 31], concerning the indirect mechanism of DR being dominated by complex resonances, may also be relevant for rotationally-autoionizing states in addition to the originally-postulated situation of vibrationally-autoionizing Rydberg states. It is beyond the scope of this study to examine this point in greater detail, but this point is worth exploring in future research.

The results presented above analyze the DR of rotationally and vibrationally cold, ground-state ^4HeH . To compare with current experiments, we must account for the nonzero temperature of the ion source. We Boltzmann-average over the population of rovibrational states at 800°K , to account for the experimental parameters of Ref.[14], and show the results for the various isotopologues in Fig. 5. We compare with the theoretical results of Guberman[2], Sarpal *et al.*[28], and Takagi[14] and it seems that the present method has produced the results most closely matching the experimental data of Tanabe[14].

For calculating the high-energy DR peak, several degrees of complication may be included in the calculation, but we find that a very simple treatment is sufficient to approximate the experimental results. We include neither the energy dependence nor the R-dependence of the fixed-nuclei S-matrix, evaluating it at 0.6 hartree and $1.6a_0$, roughly at the center of the experimentally observed peak and ground-state vibrational wavefunction.

Results for the high-energy DR calculation are shown in Fig. 6. We compare our MQDT results to the prior theoretical results of Ref. [15] and the experiments of Refs. [9] and [13]. We also calculate a result using the O'Malley framework [21] in which we first find the resonance positions and widths as a function of nuclear geometry. We do so by applying the MQDT channel-closing formula, Eq.(9), to the calculated MQDT S-matrices to obtain the "physical" S-matrix $\mathcal{S}(E)$ in the complex-energy plane. We then locate its poles $E_R^{(i)} - i\frac{\Gamma^{(i)}}{2}$. We find six resonances, $i = 1 - 6$, all of which have sigma symmetry. Using the approximate formula [21] valid for small widths,

$$\sigma(E) = \sum_i \frac{\pi^2}{E} \frac{\Gamma^{(i)}(R_i(E))}{|E_R^{(i)'}(R_i(E))|} |\Psi(R_i(E))|^2, \quad (12)$$

where the widths $\Gamma^{(i)}$, resonance energies $E_R^{(i)}$, and the ground-state vibrational wavefunction Ψ are evaluated at a geometry $R_i(E)$ consistent with a vertical transition such that $E_0 + E = E_R^{(i)}(R_i(E))$, with E_0 the initial state energy, we obtain a result consistent with our MQDT result. In the lower panel of Fig. 6 we show the contributions for each of the six sigma resonances to the total. Orel *et al.*[15] found two Π resonances having significant contribution to the total cross section, and their six Σ

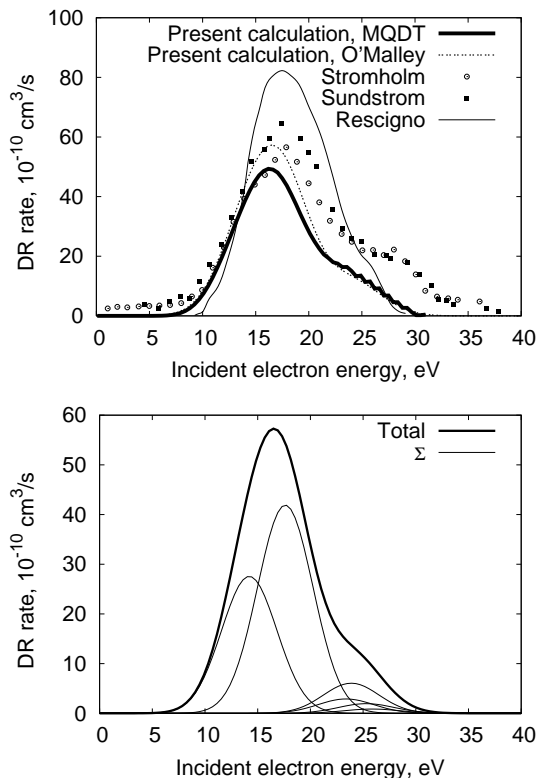


FIG. 6: **Top:** High-energy dissociative recombination rate coefficient calculated with the present MQDT treatment, compared with our results using calculated resonance curves and the O'Malley treatment (Eq.(12)), the theoretical results of Orel *et al.*[15], and the experimental results of Sundstrom *et al.* [9] and Stromholm *et al.* [13]. **Bottom:** Contribution of each of the six sigma resonances to our total result using the O'Malley treatment.

resonances give partial cross sections different from ours shown in Figure 6.

V. DISCUSSION

We have applied the theory of Ref. [1] to the calculation of DR rates for $\text{HeH}^+ + e^-$ in both the low- and high-energy regions. We have achieved very good agreement with experiment – at least as good as that of Orel *et al.* [15] for the high-energy peak, and better than all prior calculations for the low-energy region. Thus, it is clear that the present methodology gives accurate results for both the indirect and direct mechanisms.

Our treatment of the high-energy peak was perhaps the simplest possible: we used a quantum defect matrix constant with respect to both incident electron energy and internuclear radius. Such a simple treatment is applicable to much larger systems, as it leads to a sparse system of linear equations in the channel closing step, which is the rate limiting step for polyatomic DR calculations.

However, for larger systems it may be necessary to include the energy dependence of the quantum defect in order to reproduce the relevant physics of DR or rovibrational autoionization. For instance, larger polyatomic systems such as NO_2^+ will in general support a greater number of shape resonances than smaller diatomic systems, and these will impart energy-dependence to the quantum defect functions that is difficult to analytically remove.

Methods suited to a MQDT treatment including the energy dependence of the fixed-nuclei quantum defect include those of Refs.[51, 52]. These calculations require not the S-matrix but other entities such as the square root of the S-matrix or the quantum defect matrix. Therefore, such a calculation is more difficult owing to the necessity of following the branches of the quantum defect matrix across both R and E , for a large (> 1 hartree) energy range.

Even for the relatively small HeH^+ system, the high-

energy DR peak spans a large energy range and involves a large transfer of energy from the electronic to the nuclear degrees of freedom. Given these qualities, it is not *a priori* obvious that our simple treatment would accurately reproduce the physical results. We pursued an energy-dependent treatment along the lines of [52], and this was yielding results similar to those presented in Fig.6, but was not numerically stable, and would require improvement to yield publishable results.

VI. ACKNOWLEDGMENTS

We thank A. E. Orel for helpful suggestions and encouragement. This work was supported in part by the DOE Office of Science and by NSF grant number ITR 0427376, and one of us (CHG) received partial support from the Alexander von Humboldt Foundation.

-
- [1] E. L. Hamilton and C. H. Greene, Phys. Rev. Lett. **89**, 263003 (2002).
 - [2] S. L. Guberman, Phys. Rev. A **49**, R4277 (1994).
 - [3] A. I. Florescu-Mitchell and J. B. A. Mitchell, Physics Reports **430**, 277 (2006).
 - [4] M. Larsson, Annu. Rev. Phys. Chem. **48**, 151 (1997).
 - [5] J. M. Moorhead, R. P. Lowe, J. P. Maillard, W. H. Wehlau and P. F. Bernath Astrophys. J. **326**, 326 (1988).
 - [6] W. Roberge and A. Dalgarno Astrophys. J. **255**, 489 (1982).
 - [7] F. B. Yousif and J. B. A. Mitchell, Phys. Rev. A **40**, 4318 (1989).
 - [8] T. Tanabe, I. Katayama, N. Inoue, K. Chida, Y. Arakaki, T. Watanabe, M. Yoshizawa, S. Ohtani, and K. Noda, Phys. Rev. Lett. **70**, 422 (1993).
 - [9] G. Sundstrom *et al.*, Phys. Rev. A **50**, R2806 (1993).
 - [10] T. Tanabe *et al.*, Phys. Rev. A **49**, R1531 (1994).
 - [11] J. R. Mowat, H. Danared, G. Sundstrom, M. Carlson, L. Andersen, L. Vejby-Christensen, M. af Ugglas, and M. Larsson, Phys. Rev. Lett. **74**, 50 (1995).
 - [12] J. Semaniak *et al.*, Phys. Rev. A **54**, R4617 (1996).
 - [13] C. Stromholm, J. Semaniak, S. Rosen, H. Danared, S. Datz, W. van der Zande, and M. Larsson, Phys. Rev. A **54**, 3086 (1996).
 - [14] T. Tanabe, I. Katayama, S. Ono, K. Chida, T. Watanabe, Y. Arakaki, Y. Haruyama, M. Saito, T. Odagiri, K. Hosono, *et al.*, J. Phys. B **31**, L297 (1998).
 - [15] A. E. Orel, K. C. Kulander, and T. N. Rescigno, Phys. Rev. Lett. **74**, 4807 (1995).
 - [16] A. Larson and A. E. Orel, Phys. Rev. A **72**, 032701 (2005).
 - [17] S. Morisset, L. Pichl, A. E. Orel, and I. F. Schneider, Phys. Rev. A **76**, 042702 (2007).
 - [18] H. Takagi, Phys. Rev. A **70**, 022709 (2004).
 - [19] H. Takagi, J. Phys. Conf. Ser. **4**, 155 (2005).
 - [20] D. R. Bates, Phys. Rev. **78**, 492 (1950).
 - [21] T. F. O'Malley, Phys. Rev. **150**, 14 (1966).
 - [22] M. J. Seaton, Rep. Prog. Phys. **46**, 167 (1983).
 - [23] U. Fano, Phys. Rev. A **2**, 353 (1970).
 - [24] E. S. Chang and U. Fano, Phys. Rev. A **6**, 173 (1972).
 - [25] C. Greene, U. Fano, and G. Strinati, Phys. Rev. A **19**, 1485 (1979).
 - [26] C. H. Greene, A. R. P. Rau, and U. Fano, Phys. Rev. A **26**, 2441 (1982).
 - [27] A. Gusti, J. Phys. B **13**, 3867 (1980).
 - [28] B. K. Sarpal, J. Tennyson, and L. A. Morgan, J. Phys. B **27**, 5943 (1994).
 - [29] V. Kokouline and C. H. Greene, Phys. Rev. A **68**, 012703 (2003).
 - [30] R. Curik and C. H. Greene, Phys. Rev. Lett. **98**, 173201 (2007).
 - [31] R. Curik and C. H. Greene, Mol. Phys. **105**, 1565 (2007).
 - [32] O. I. Tolstikhin, V. N. Ostrovsky, and H. Nakamura, Phys. Rev. A **58**, 2077 (1998).
 - [33] A. Jackle and H.-D. Meyer, J. Chem. Phys. **105**, 6778 (1996).
 - [34] C. Leforestier and R. E. Wyatt, J. Chem. Phys. **78** (1983).
 - [35] R. Kosloff and D. Kosloff, J. Comput. Phys. **63** (1986).
 - [36] J. Aguilar and J. M. Combes, Commun. Math. Phys. **22**, 269 (1971).
 - [37] E. Balslev and J. M. Combes, Commun. Math. Phys. **22**, 280 (1971).
 - [38] N. Moiseyev, P. R. Certain, and F. Weinhold, Mol. Phys. **36**, 1613 (1978).
 - [39] N. Moiseyev and J. O. Hirschfelder, J. Chem. Phys. **88**, 1063 (1987).
 - [40] N. Lipkin, R. Lefebvre, and N. Moiseyev, Phys. Rev. A **45**, 4553 (1992).
 - [41] N. Moiseyev, Physics Reports **302**, 211 (1998).
 - [42] C. W. McCurdy, M. Baertschy, and T. N. Rescigno, J. Phys. B **37**, R137 (2004).
 - [43] J. Tennyson and L. A. Morgan, Phil. Trans. R. Soc. Lond A **357**, 1161 (1999).
 - [44] A. D. McLean, M. Yoshimine, B. H. Lengsfeld, P. S. Bagus, and B. Liu, in *Modern Techniques in Computational Chemistry 1991, MOTTECC 91*, edited by E. Clementi (Elsevier B.V., Leiden, 1991), p. 233.

- [45] F. Alexandre, J. D. Gorfinkiel, L. A. Morgan, and J. Tennyson, *Computer Physics Communications* **144**, 224 (2002).
- [46] H.-J. Werner, P. J. Knowles, R. Lindh, F. R. Manby, M. Schütz, P. Celani, T. Korona, A. Mitrushenkov, G. Rauhut, T. B. Adler, et al., *Molpro, version 2006.1, a package of ab initio programs* (2006), see <http://www.molpro.net>.
- [47] T. N. Rescigno and C. W. McCurdy, *Phys. Rev. A* **62**, 032706 (2000).
- [48] M. Pavanello and S. Bubin, *J. Chem. Phys.* **123**, 104306 (2005).
- [49] J. A. Coxon and P. G. Hajigeorgiou, *J. Mol. Spectroscopy* **193**, 306 (1999).
- [50] D. M. Bishop and L. M. Cheung, *J. Mol. Spectroscopy* **75**, 462 (1979).
- [51] C. H. Greene and C. Jungen, *Phys. Rev. Lett.* **55**, 1066 (1985).
- [52] H. Gao and C. H. Greene, *J. Chem. Phys* **91**, 3988 (1989).